

Numerical Simulation of Molecularly Thin Lubricant Film Flow Due to the Air Bearing Slider in Hard Disk Drives

Hiroyuki Kubotera
Visiting industrial fellow
Department of Mechanical Engineering
University of California at Berkeley
kubotera@cml.me.berkeley.edu

David B. Bogy
William S. Floyd, Jr. Distinguished Professor in Engineering
Department of Mechanical Engineering
University of California at Berkeley
dbogy@cml.me.berkeley.edu

Abstract

In this paper, we numerically study the evolution of depletion tracks on molecularly thin lubricant films due to a flying head slider in a hard disk drive. Here the lubricant thickness evolution model is based on continuum thin film lubrication theory with inter-molecular forces. Our numerical simulation involves air bearing pressure, air bearing shear stress, Laplace pressure, the dispersive component of surface free energy and disjoining pressure, a polynomial modeled polar component of surface free energy and disjoining pressure and shear stress caused by the surface free energy gradient. Using these models, we perform the lubricant thickness evolution on the disk under a two-rail taper flat slider. The results illustrate the forming process of two depletion tracks of the thin lubricant film on the disk. We also quantify the relative contributions of the various components of the physical models. We find that the polar components of surface free energy and disjoining pressure and the shear stress due to the surface free energy gradient, as well as other physical models, play important rolls in thin lubricant film thickness change.

1. Introduction

Experimental measurements have shown that a very low flying head slider makes depletion tracks

on a thin lubricant film [1-4]. Numerical modeling of this phenomenon is important in order to achieve higher data densities that require ultra low flying height sliders that carry the read-write transducers. Various authors have reported numerical simulations that have been carried out for this purpose using continuum thin film lubrication theory [1, 5-8]. Pouwer et al. performed lubricant depletion track simulations due to air bearing shear stress for a 2-rail taper flat slider [1]. Yorino et al. performed a 3-dimensional lubricant flow simulation including air bearing pressure, air bearing shear stress, and Laplace pressure [6]. Yanagisawa et al. performed lubricant flow simulations taking into account air bearing shear stress, outside slider air shear stress and diffusion terms [7]. Wu performed 3-dimensional lubricant flow simulations with air bearing pressure, air bearing shear stress, outside the slider air shear stress, Laplace pressure and disjoining pressure [8].

Recently, polar end-group terminated perfluoropolyether (PFPE) lubricants have been used for hard disk drives. The effect of the polar components on the surface free energy and disjoining pressure is relatively large and may not be negligible in lubricant depletion. But, the effect of the polar component of the surface free energy and disjoining pressure, and the shear stress caused by the surface free energy gradient to lubricant tracks are still not well understood. Furthermore, the relative contributions of related physical models have not been quantified.

In this paper we perform numerical simulations of molecularly thin lubricant film flow that involve air bearing pressure, air bearing shear stress, Laplace pressure, the dispersive component of the surface free energy and disjoining pressure, the polynomial modeled polar component of surface free energy and disjoining pressure and shear stress caused by the surface free energy gradient. We also quantify the contributions of these physical models to the lubricant thickness change.

2. Governing equations and Numerical Method

The governing equations for thin lubricant film flow and the numerical method used here are basically those of Yorino et al. [6]. Based on long wave theory [9], the lubricant thickness evolution is determined by equation (1) [5-6]. Here h_L is the lubricant thickness, μ_L is the lubricant viscosity, p_L is the lubricant pressure, τ_L is the lubricant shear stress, and u is the disk velocity. In equation (1) below the spatial gradient terms correspond to the flow caused by the x-directional pressure gradient, x-directional shear stress, x-directional disk velocity, and the y-directional pressure gradient, y-directional shear stress and y-directional disk velocity, respectively.

$$\begin{aligned}
& \frac{\partial h_L}{\partial t} - \frac{1}{3\mu_L} \frac{\partial}{\partial x} \left(\frac{\partial p_L}{\partial x} h_L^3 \right) + \frac{1}{2\mu_L} \frac{\partial}{\partial x} (\tau_{Lx} h_L^2) + u_x \frac{\partial h_L}{\partial x} \\
& - \frac{1}{3\mu_L} \frac{\partial}{\partial y} \left(\frac{\partial p_L}{\partial y} h_L^3 \right) + \frac{1}{2\mu_L} \frac{\partial}{\partial y} (\tau_{Ly} h_L^2) + u_y \frac{\partial h_L}{\partial y} = 0
\end{aligned} \tag{1}$$

Considering the force and stress balance at the lubricant surface, the lubricant pressure and shear stress are given by equations (2), (3), where p_G is the air bearing pressure, Π_{dis} and Π_{pol} are dispersive and polar components of the disjoining pressure, γ_{dis} and γ_{pol} are dispersive and polar components of surface free energy, and τ_G is the air bearing shear stress. Here, the fourth term of equation (2) is the Laplace pressure term. The second and third terms of equation (3) are shear stress caused by the surface free energy gradient [6].

$$p_L = p_G - \Pi_{dis} - \Pi_{pol} - (\gamma_{dis} + \gamma_{pol}) \left(\frac{\partial^2 h_L}{\partial x^2} + \frac{\partial^2 h_L}{\partial y^2} \right) \tag{2}$$

$$\tau_{Lx} = \tau_{Gx} + \frac{\partial \gamma_{dis}}{\partial x} + \frac{\partial \gamma_{pol}}{\partial x}, \quad \tau_{Ly} = \tau_{Gy} + \frac{\partial \gamma_{dis}}{\partial y} + \frac{\partial \gamma_{pol}}{\partial y} \tag{3}$$

The dispersive component of surface free energy is modeled by equation (4), where γ_∞ is the surface free energy of the bulk liquid, c_i is the coefficient of the dispersive component of surface free energy, d_0 is a characteristic length in the film thickness direction. The first term corresponds to a constant term and the second term corresponds to the van der Waals attractive term.

$$\gamma_{dis} = \gamma_\infty \left(c_0 + \frac{c_1}{(h/d_0)^2} \right) \tag{4}$$

The polar component of surface free energy is modeled by equation (5). Various experimental measurements of surface free energy of polar end-group terminated PFPE lubricants have been carried out [10-11]. Those measurements showed that the polar component of the surface free energy oscillates with the film thickness. In order to represent precise surface free energy profiles, we model the polar component of surface free energy by certain polynomial equations [12] in this study.

$$\gamma_{pol} = \gamma_\infty \sum_{i=0}^n a_i (h/d_0)^i \tag{5}$$

The dispersive and polar components of the disjoining pressure are defined by equation (6).

$$\Pi_{dis} = -\frac{\partial \gamma_{dis}}{\partial h_l}, \quad \Pi_{pol} = -\frac{\partial \gamma_{pol}}{\partial h_l} \tag{6}$$

The air bearing governing equation is the MGL equation (7) [15], where h_G is the air bearing spacing, μ_G is air viscosity and Q is a flow factor.

$$\begin{aligned} \frac{\partial(p_G h_G)}{\partial t} - \frac{1}{12\mu_G} \frac{\partial}{\partial x} \left(Q p_G h_G^3 \frac{\partial p_G}{\partial x} \right) + \frac{1}{2} u_x \frac{\partial}{\partial x} (p_G h_G) \\ - \frac{1}{12\mu_G} \frac{\partial}{\partial y} \left(Q p_G h_G^3 \frac{\partial p_G}{\partial y} \right) + \frac{1}{2} u_y \frac{\partial}{\partial y} (p_G h_G) = 0 \end{aligned} \quad (7)$$

The air bearing shear stress is calculated by equation (8).

$$\tau_{Gx} = \frac{h_G}{2} \frac{\partial p_G}{\partial x} - \frac{\mu_G u_x}{2a\lambda + h_G}, \quad \tau_{Gy} = \frac{h_G}{2} \frac{\partial p_G}{\partial y} - \frac{\mu_G u_y}{2a\lambda + h_G} \quad (8)$$

The governing equations (1)-(8) are strongly nonlinear and must be solved numerically. Equation (1) was divided into its advection phase and non-advection phase by the time splitting method. The advection phase was discretized by a CIP (Cubic-Interpolated Propagation) scheme type C [13], and the non-advection phase was discretized by an implicit finite volume method [14]. We applied the ADI (Alternating Direction Implicit) method and the Newton-Raphson method for the non-advection phase. An unequally-spaced mesh was used. The air bearing pressure and shear stress were calculated using equations (7), (8) with CMLAir [16-17] which has been developed at the Computer Mechanics Laboratory at UC Berkeley.

3. Simulation Conditions

Fig.1 shows a schematic diagram of the configuration. The slider is a 2 rail taper flat positive pressure nano size slider. Realizing that more complex ABS designs are currently required in HDDs we nevertheless use this simple ABS here to focus on the relative contributions of the various models. The flying height, pitch angle and roll angle are 10 nm, $150 \mu rad$, $0 \mu rad$ respectively. The disk rotation speed is 5,400 rpm. The radial position of the flying slider is 10 mm. The initial lubricant thickness is 1.25 nm. The width and length of the lubricant computational region are 3.0 mm and 62.8 mm, respectively. The length of the computational region corresponds to the length of the circular track. In order to reproduce a looped track we apply periodic boundary conditions to both ends of the computational region. The lubricant is the polar end-group terminated perfluoropolyether (PEPE) Z-DOL with viscosity coefficient 0.144 Pas [5] and surface free energy parameters as listed in Table 1, and as reported by Karis et al. [12]. Fig.2 shows the dispersive and polar components of

the surface free energy as functions of the lubricant film thickness. Fig.3 shows the dispersive and polar components of the disjoining pressure as functions of thickness. As seen in these figures the polar component of the surface free energy and disjoining pressure oscillate with lubricant film thickness. The contributions of the polar components are relatively large and definitely are not negligible.

4. Simulation Results and Discussion

4.1 With all physical models included

Fig.4 shows the air bearing surface geometry, air bearing pressure and air bearing shear stress. The bottom side of the figures corresponds to the inner side. The maximum pressure is 13.8 atmospheres, and the maximum shear stress in the length direction is 0.0083 atmospheres. The maximum shear stress in the width direction is 0.0020 atmospheres. Compared with pressure the shear stress is small, but, as we will explain later, the shear stress has a dominant effect on lubricant flow.

Near the edge of the rail the width directional shear stresses are relatively large. Near the outer edge of the rails, the width directional shear stresses are positive (outer direction). Near the inner edge of the rails, the width directional shear stresses are negative (inner direction). These shear stresses are the dominant cause of the depletion tracks on the thin lubricant films.

Fig.5 shows the simulation results for the lubricant thickness profiles near the slider in the incipient period. The initial lubricant thickness was uniform (Fig.5 (a)). After $1 \mu\text{sec}$ of slider flying, lubricant depletion and build-up occurred near the rails of the slider, because the air bearing pressure and shear stress pushed aside the lubricant (Fig.5 (b)). As time proceeded, the lubricant depletion and build-up region moved downstream due to the disk rotation (Fig.5 (c)). After about 1 revolution of the disk the depletion and build-up region runs into the slider region again (Fig.5 (d)). Lubricant is pushed aside again by the air bearing pressure and shear stress. Because these processes act repeatedly, the lubricant depletion tracks evolve.

Fig.6 shows the time evolution of the lubricant thickness profiles in the radial direction section. The circumferential position is at the slider center. The two depletion regions correspond to the two rails of the slider. Because the air bearing pressure is imposed repeatedly, the amount of depletion and build-up increases with time. Fig.7 shows the time evolution of the lubricant thickness profiles in a circumferential direction section. The radial position is at the inner rail center which corresponds

to the valley of lubricant thickness in Fig.6. The slider position is shown in this figure. The lubricant thickness change in the circumferential direction is small compared to that in radial direction.

Fig.8 shows the lubricant thickness profile after a slider flew for 5 minutes on the same track. This figure shows the whole track lubricant thickness profile. The horizontal axis corresponds to the circumference, ranging from 0 to 360 degrees. The total length in the circumferential direction is 62.8mm. Two depletion tracks are clearly observed on the lubricant film in Fig.8. Their locations correspond to the rails of the slider.

4.2 Quantitative contribution of the physical models

We also investigated the contributions of the various physical models to the lubricant thickness change. Air bearing pressure, air bearing shear stress, Laplace pressure, the dispersive component of surface free energy and disjoining pressure, the polynomial modeled polar component of surface free energy and disjoining pressure and shear stress caused by the surface free energy gradient were all included in the simulation. Next, in order to quantify the contributions of the various physical models, we removed their corresponding terms from the simulation equation sequentially.

Fig.9 shows cross-sectional profiles of the lubricant thickness after 5 min of slider flying. In this figure the result with all of the physical models, the result without the air bearing pressure and the result without the air bearing shear stress are shown. The result with all physical models and the result without the air bearing pressure are close to each other. So the contribution of air bearing pressure to the lubricant thickness change is small. Next, without the air bearing shear stress it is seen that the lubricant thickness change is very small. So the contribution of air bearing shear stress to lubricant thickness change is relatively large.

Fig.10 also shows cross-sectional profiles of the lubricant thickness after 5 min of slider flying. In this figure, the result with all physical models and the results without some of the physical models are shown. The result without Laplace pressure and the result with all physical models are quite close. So, the contribution of Laplace pressure to lubricant thickness change is small. This is because the radius of curvature of the lubricant surface is relatively large and surface free energy of the lubricant is relatively small. The Laplace pressure, which can be obtained by dividing the surface free energy by the radius of curvature, is small. Consequently, the Laplace pressure has a minor

effect on lubricant thickness change. The results without the dispersive component and the results with all physical models are different. So, the dispersive component has an important effect on the lubricant thickness change. The result without shear stress caused by the surface free energy gradient and the result with all physical models are different. So, the shear stress caused by the surface free energy gradient also has an important effect on the lubricant thickness change.

In Fig.10 the result without the polar component and the result with all physical models are quite different. Without the polar component the profile shows sharp peaks [8], but when including the polar components of surface free energy and disjoining pressure the sharp peaks did not emerge. So, we confirmed that these polar components have a dominant effect on the lubricant thickness change. Especially seen is that the polar component reduces the sharp peaks. The reduced sharp peak profile corresponds more closely to experimental measured lubricant thickness profiles [1-4].

From these results, we confirmed the following: 1) The air bearing shear stress has a dominant effect on lubricant film thickness change [8]. 2) The air bearing pressure has a minor effect on lubricant film thickness change [8]. 3) The polar component has a dominant effect on lubricant film thickness change in our simulated condition. 4) The shear stress caused by the surface free energy gradient and dispersive component have certain significant effects on the lubricant thickness change. 5) Laplace pressure has a minor effect on lubricant thickness change.

5. Conclusions

We performed numerical simulations of a molecularly thin lubricant film flow due to a slider flying in a hard disk drive. Our numerical simulation included air bearing pressure, air bearing shear stress, Laplace pressure, the dispersive component of surface free energy and disjoining pressure, the polynomial modeled polar component of surface free energy and disjoining pressure and shear stress caused by surface free energy gradient. Using those models, we performed the lubricant film thickness evolution on the disk under a two rail taper flat slider. The results illustrate the forming process of two depletion tracks of the thin lubricant film on the disk. We also quantified the contributions of the related physical models. We found that air bearing shear stress, the polar component of surface free energy and disjoining pressure and shear stress by surface free energy gradient as well as other physical models play important rolls in the thin lubricant film thickness change.

The lubricant flow simulation under modern negative pressure type sliders and comparison with the experimental results will be the topic of a future paper...

References

- [1] Power, A., Kawakubo, Y., and Tsuchiyama, R., 2001, "Lubricant Flow under a Flying Head on a Thin-Film Disk", IEEE Transactions on Magnetics, vol. 37, No.4, 1869-1871.
- [2] Ma, X., Tang, H., Stirniman, M., and Gui, J., 2002, "Lubricant Thickness Modulation Induced by Head-Disk Dynamic Interactions", IEEE Transactions on Magnetics, vol. 38, No.1, 112-117.
- [3] Ma, X., Kuo, D., Chen, J., Tang, H., and Gui, J., 2002, "Effect of Lubricant on Flyability and Read-Write Performance in the Ultra-Low Flying Regime", Journal of Tribology, Vol. 124, 259-265.
- [4] Deoras, S. K., and Talke, F. E., 2003, "Slider-Lubricant Interactions for Low Flying Sliders", IEEE Transactions on Magnetics, vol. 39, No. 5, 2471-2473.
- [5] Yorino, K., Konishi, N., Yamane, K., Matsuoka, H., and Fukui, S., 2004, "Lubricant deformation using long wave equation", Proc. of JSME Mechanical Engineering Congress, 371-372 (in Japanese)
- [6] Yorino, K., Konishi, N., Yamane, K., Matsuoka, H., and Fukui, S., 2004, Proc. of JAST Tribology Conference (in Japanese)
- [7] Yanagisawa, K., Kawakubo, Y., and Yoshino, M., 2005, "Effects of diffusion on lubricant distribution under flying head on thin-film disks", Tribology Letters, Vol.18, No.1, 113-117.
- [8] Wu, L., 2005, "Lubricant Depletion Due To Slider-Lubricant Interaction In Hard Disk Drives", ASME Proc. of 15th Annual Conference on Information Storage and Processing Systems.
- [9] Oron, A., Davis, S. H., Bankoff, S. G., 1997, "Long-scale evolution of thin liquid films", Reviews of Modern Physics, Vol. 69, No. 3, 931-980.
- [10] G.W. Tyndall, P.B. Leezenberg, R.J. Waltman, J. Castenada, 1998, "Interfacial interactions of perfluoropolyether lubricants with magnetic recording media", Tribology Letters, vol. 4, 103-108.
- [11] R.J. Waltman, D. Pocker, G.W. Tyndall, 1998, "Studies on the interactions between ZDOL perfluoropolyether", Tribology Letters, vol. 4, 267-275.
- [12] Karis, T. E., and Tyndall, G. W., 1999, "Calculation of spreading profiles for molecularly-thin films from surface energy gradients," J. Non-Newtonian Fluid Mech., 82, 287-302.

- [13] Aoki, T., 1995, "Multi-dimensional advection of CIP (Cubic-Interpolated propagation) scheme", *Computational Fluid Dynamics Journal*, vol.4, no.3, 279-291.
- [14] Patankar, S. V., 1980, *Numerical Heat Transfer and Fluid Flow*, McGraw-Hill, New York.
- [15] Fukui, S., and Kaneko, R., 1995, "Molecular Gas Film Lubrication", in *Handbook of Micro/Nanotribology*, edited by B. Bhushan, CRC Press, 559-603.
- [16] Lu, S., 1997, "Numerical Simulation of Slider Air Bearings", *Doctoral Dissertation*, University of California at Berkeley.
- [17] Lu, S., Hu, Y., O'Hara M., Bogy, D. B, Bhatia, S., Hsia, Y., 1996, "Air Bearing Design, Optimization, Stability Analysis and Verification for sub-25 nm Flying", *IEEE Transactions on Magnetics*, vol. 32, No.1, 103-109.

Parameters	Dispersive	Polar
$d_0 = 0.4 \text{ nm}$	$c_0 = 0.6144$	$a_0 = 0.35634428$
$\gamma_\infty = 26 \text{ mN/m}$	$c_1 = 0.1508$	$a_1 = 0.943984495$
		$a_2 = -1.09056649$
		$a_3 = 0.493599274$
		$a_4 = -0.10894144$
		$a_5 = 0.0125571518$
		$a_6 = -7.28088361 \times 10^{-4}$
		$a_7 = 1.68021545 \times 10^{-5}$

Table.1 Surface free energy parameters.

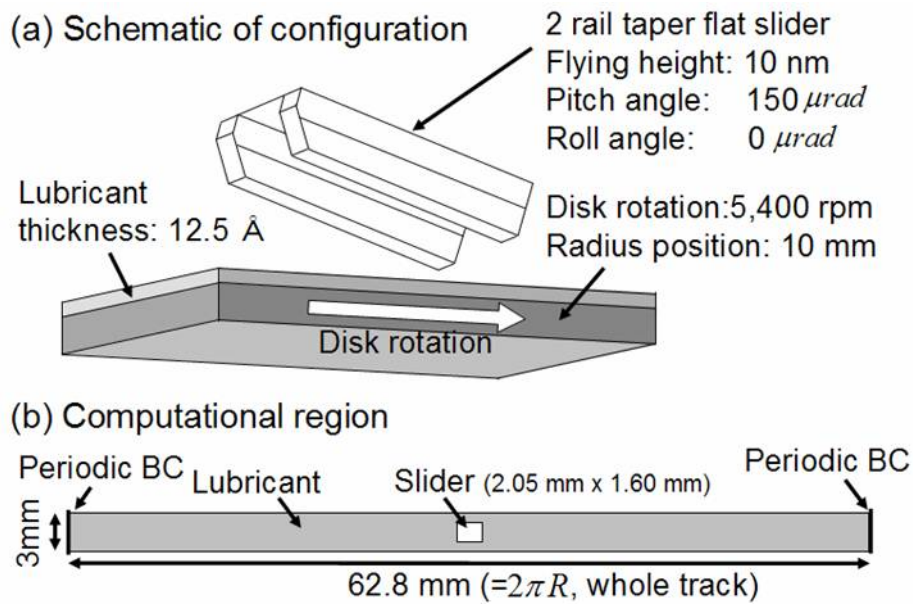


Fig.1 Schematic diagram of the configuration.

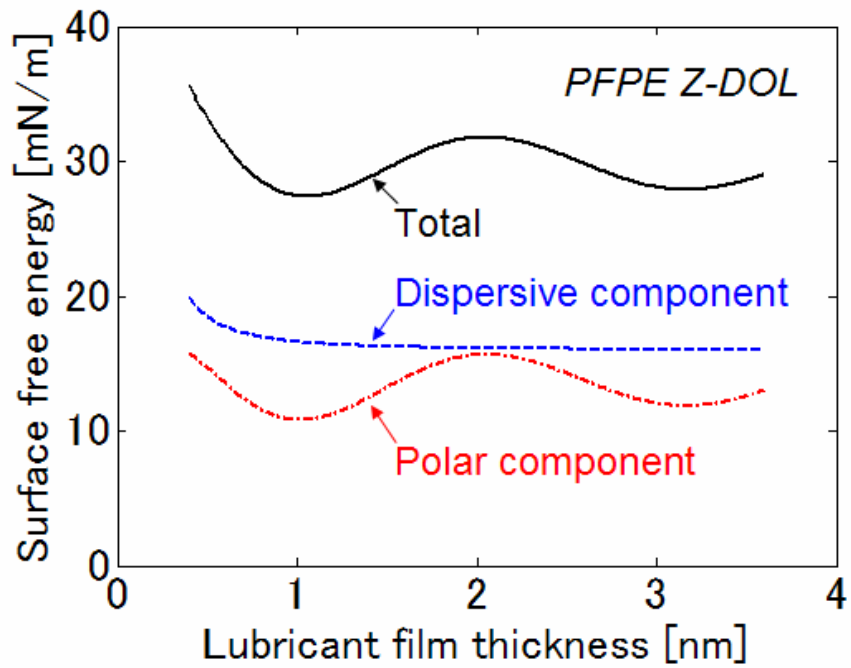


Fig.2 Surface free energy profiles used in the numerical simulations. These profiles were reported by Karis et al. [12].

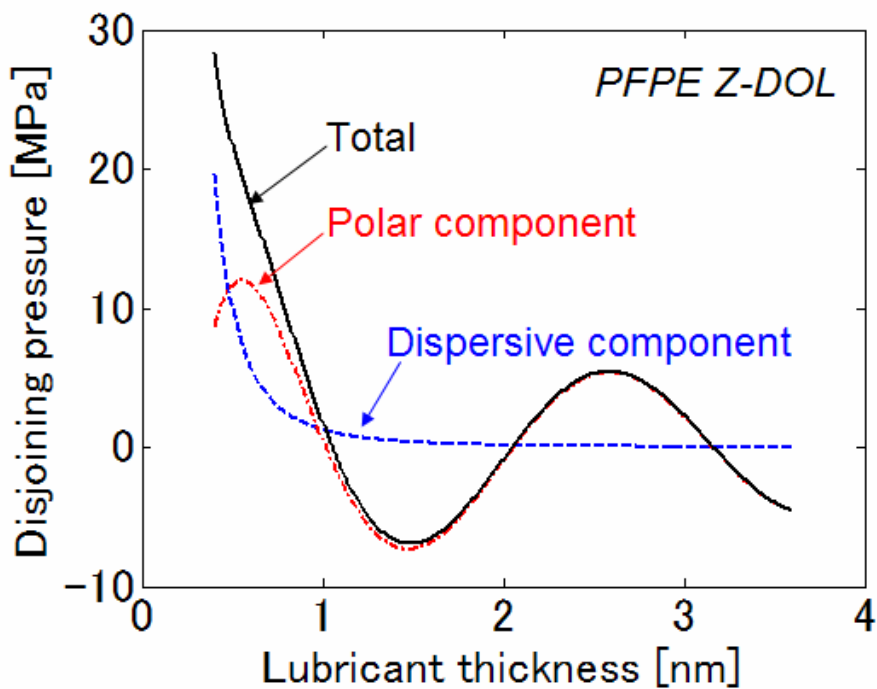


Fig.3 Disjoining pressure profiles used in the numerical simulations. These profiles were reported by Karis et al. [12].

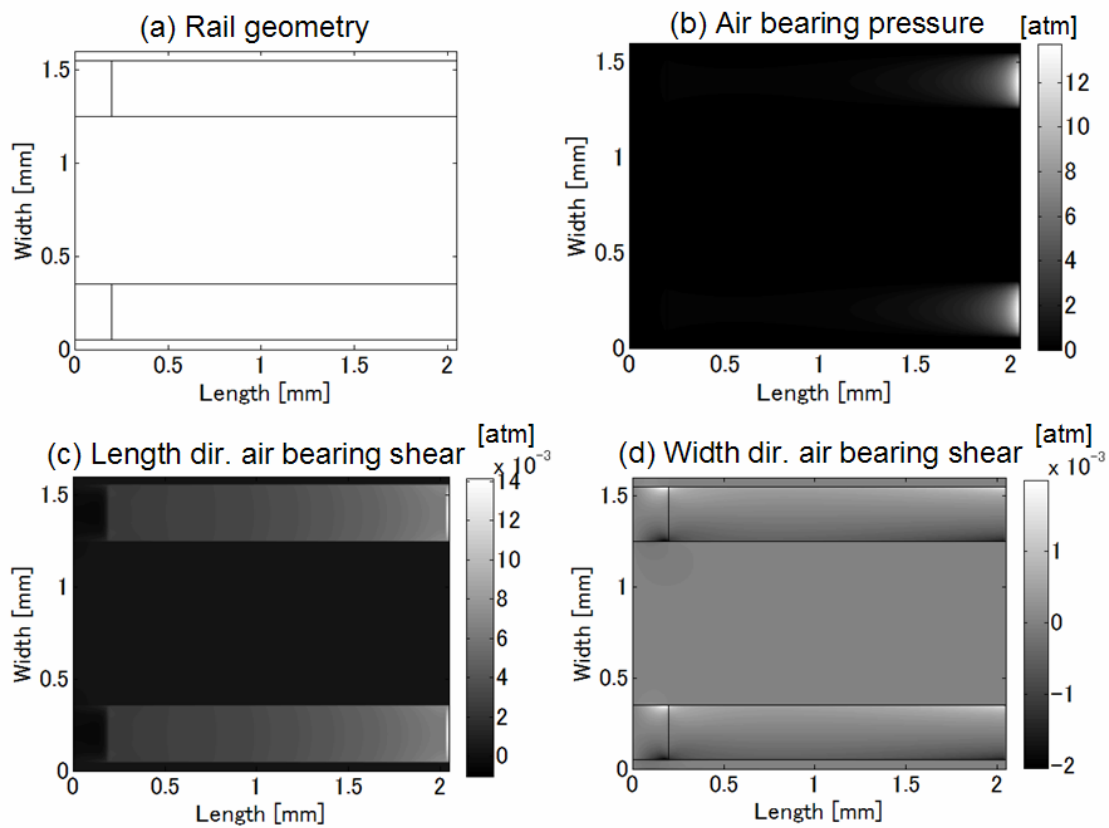


Fig.4 Air bearing pressure and shear stress.

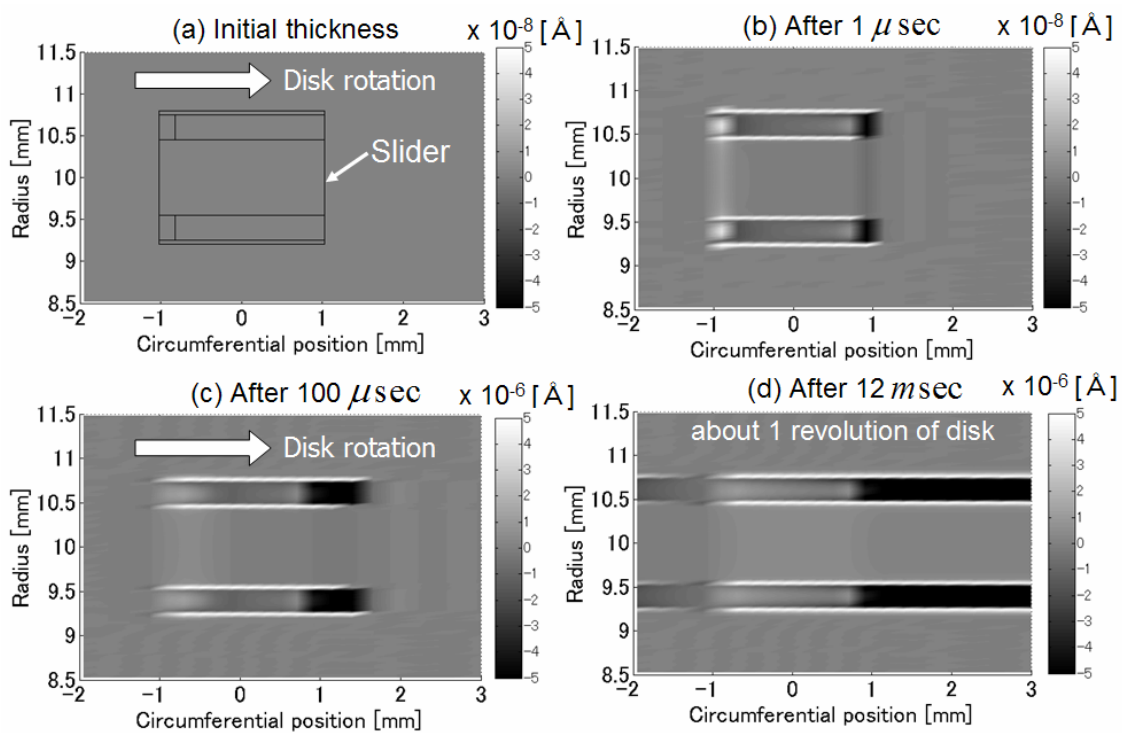


Fig.5 Lubricant thickness in the incipient period.

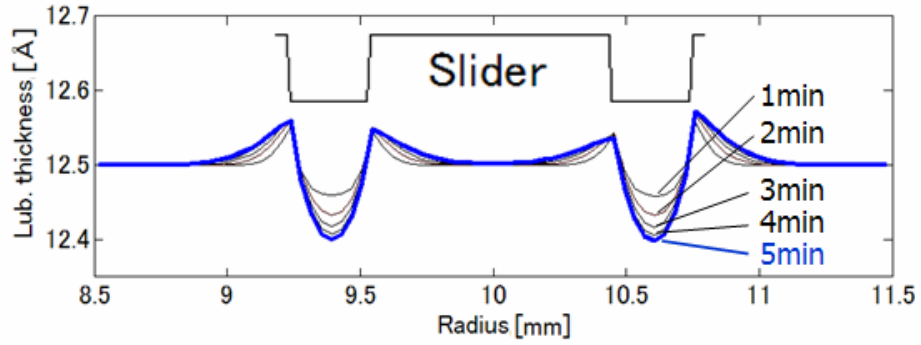


Fig.6 Time evolution of lubricant thickness profiles in a radial direction section.

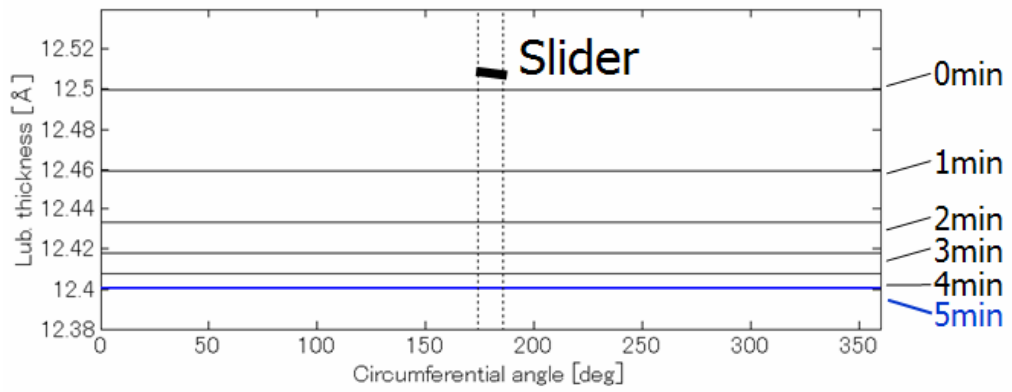


Fig.7 Time evolution of lubricant thickness profiles in a circumferential direction section.

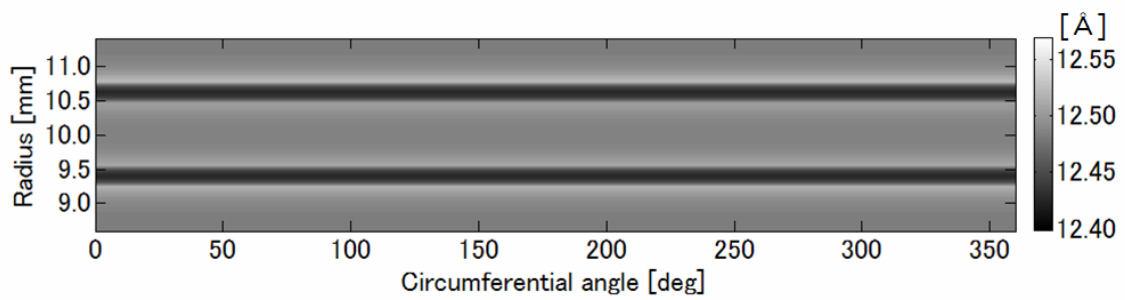


Fig.8 Lubricant thickness after the slider has flown 5 min.

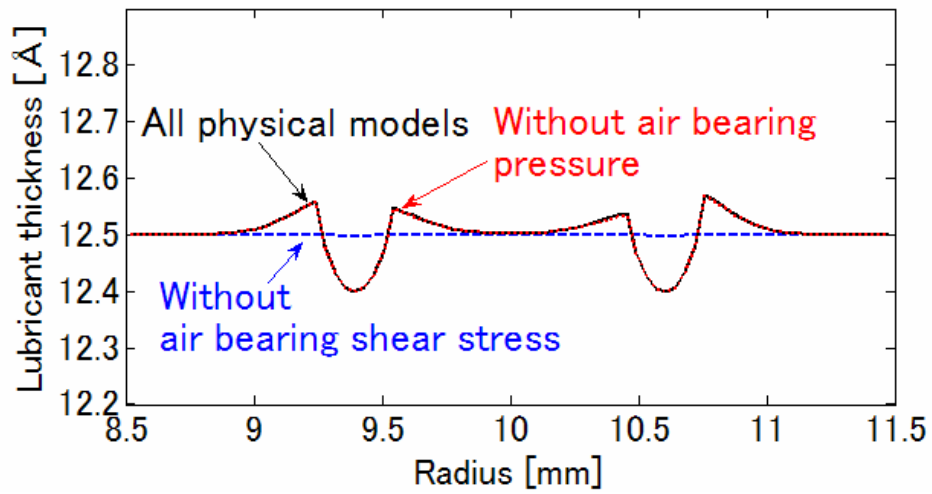


Fig.9 Contributions of the air bearing pressure and air bearing shear stress.

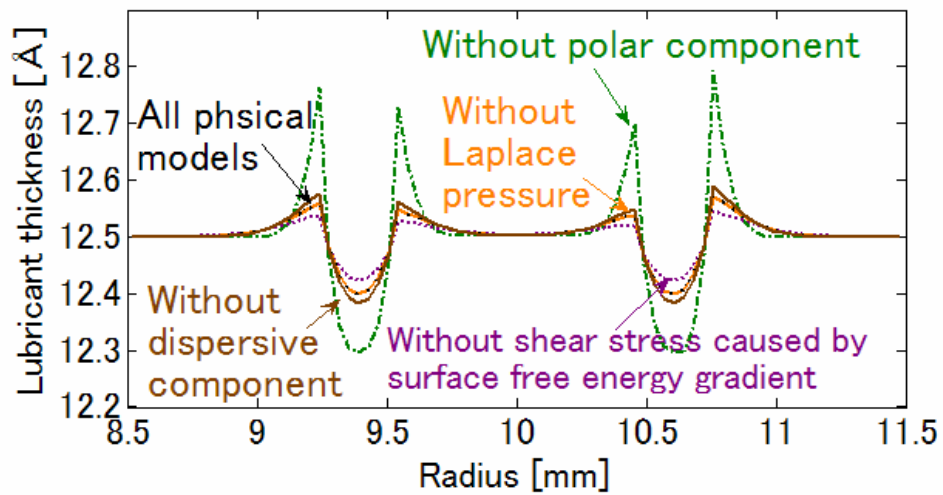


Fig.10 Contributions of the dispersive component, polar component, shear stress caused by surface free energy gradient and Laplace pressure.